Precision Measurement of the Quadrupole Coupling and Chemical Shift Tensors of the Deuterons in α-Calcium Formate

Heike Schmitt, H. Zimmermann, O. Körner, M. Stumber, C. Meinel, and U. Haeberlen

Max-Planck-Institut für Medizinische Forschung, AG Molekülkristalle, Jahnstrasse 29, 69120 Heidelberg, Germany

Using calcium formate, α-Ca(DCOO)$_2$, as a test sample, we explore how precisely deuteron quadrupole coupling (QC) and chemical shift (CS) tensors Q and σ can currently be measured. The error limits, ± 0.09 kHz for the components of Q and ± 0.06 ppm for those of σ, are at least three times lower than in any comparable previous experiment. The concept of a new receiver is described. A signal/noise ratio of 100 is realized in single-shot FT spectra. The measurement strategies and a detailed error analysis are presented. The precision of the measurement of Q is limited by the uncertainty of the rotation angles of the sample and that of σ by the uncertainty of the phase correction parameters needed in FT spectroscopy. With a 4-sigma confidence, it is demonstrated for the first time that the unique QC tensor direction of a deuteron attached to a carbon deviates from the bond direction; the deviation found is $(1.2 \pm 0.3°)$. Evidence is provided for intermolecular QC contributions. In terms of Q, their size is roughly 4 kHz. The deuteron QC tensors in α-Ca(DCOO)$_2$ (two independent deuteron sites) are remarkable in three respects. For deuterons attached to sp^2 carbons, first, the asymmetry factors η and, second, the quadrupole coupling constants C_Q, are unusually small, $\eta_1 = 0.018$, $\eta_2 = 0.011$, and $C_{Q1} = (151.27 \pm 0.06)$ kHz, $C_{Q2} = (154.09 \pm 0.06)$ kHz. Third, the principal direction associated with the largest negative QC tensor component lies *in* and not, as usual, perpendicular to the molecular plane. A rationalization is provided for these observations. The CS tensors obtained are in quantitative agreement with the results of an earlier, less precise, line-narrowing multiple-pulse study of α-Ca(HCOO)$_2$. The assignment proposed in that work is confirmed. Finally we argue that a further 10-fold increase of the measurement precision of deuteron QC tensors, and a 2-fold increase of that of CS tensors, should be possible. We indicate the measures that need to be taken. © 2001 Academic Press

Key Words: precision deuteron quadrupole coupling/chemical shift tensors; relation to *n*-structure.

INTRODUCTION

We are well aware that a precision measurement of quadrupole coupling (QC) and chemical shift (CS) tensors in a compound as simple and nonbiological as deuterated α-calcium formate, Ca(DCOO)$_2$, is against the solid-state NMR mainstream in the dawning 21st century A.D. For almost 3 decades we have measured proton and deuteron CS tensors and, for 2 decades, deuteron QC tensors, often as a necessary first step in studies

of molecular dynamics. Now, just before closing down our laboratory, we wanted to find out how precisely we can measure such tensors and what actually dominates the error limits. Perhaps not surprisingly, it turned out during this study that the increased precision allows us to address questions about which people could so far at best speculate.

In the 1980s, several research groups (*1–3* and others) started to use extensively the quadrupole moment of the deuteron to probe the structure and the dynamics of solid materials, often materials of claimed biological interest. As a rule, these groups studied powder samples. Almost invariably, their analyses of 1d and 2d (exchange) spectra involved the tacit or outspoken assumption that the QC tensor **Q** at the site of a deuteron is axially symmetric about the deuteron's bond and that the quadrupole coupling constant $C_Q = e^2 q Q/h$ (we use Slichter's notation (*4*)) is, depending on the type of bond, some value between 144 and 193 kHz (*5*). Until very recently, such assumptions were even made in cases (*6*) where the complete QC tensor **Q** had been measured before in single crystal samples (*7*). For spin-1 nuclei such as deuterons it is convenient to define the QC tensor by $\mathbf{Q} = \frac{3}{2}(eQ/h)\mathbf{V}$ where h is Planck's constant and e the (positive) elementary charge. Q is the (scalar) nuclear quadrupole moment which for deuterons is $+0.2860 \cdot 10^{-30}$ m^2 (*8*). **V** is the electric field gradient (EFG) at the site of the nucleus. This definition ensures that the separation of the components of the quadrupolar split deuteron doublet in a high-field NMR experiment is directly given by Q_{zz} where the z-direction is parallel to the applied magnetic field $\mathbf{B}_0$.

The justification of the assumptions about the shape, orientation, and size of a deuteron's QC tensor comes from three sources. The first are quantum chemical calculations which predict, for deuterons bound, e.g., to carbons, more or less axially symmetric QC tensors aligned along the deuteron's bond (*9*). With regard to the size of C_Q, the predictive power of such calculations is modest, in view of the narrow range in which C_Q is found in different compounds and in different types of bonds it is, in fact, almost worthless. The second source is just the wealth of experience that has accumulated over the course of time. There is no doubt: the assumptions work. The third source is a limited number of single crystal measurements of deuteron QC tensors done mostly, but not

exclusively, in our laboratory, and comparisons of the orientation of $\mathbf{Q}$ with structure information derived from X-ray and, in particular, neutron diffraction experiments (10–17). Generalizing, with due caution, the results of these studies, the above-quoted assumptions can be quantified in the following empirical rules (i)–(iii): First, the QC tensors of deuterons bound to carbons, oxygens, . . . , are nearly axially symmetric. Thus, rule (i) states: the asymmetry factor η (4) of such tensors remains in the range $0 \leq \eta \lesssim 0.1$. The upper end of this range tends to be approached whenever the deuteron is part of a pronounced planar structure (16, 17).

Second, because of the near-axial symmetry of $\mathbf{Q}$, this tensor has what we call a *unique principal direction*, denoted by $\mathbf{e}_Z$. It is the principal direction of $\mathbf{Q}$ which is parallel to the approximate axial symmetry axis and corresponds, consequently, to the largest principal component, Q_{ZZ}, of $\mathbf{Q}$ (by magnitude, but actually also in absolute terms (13, 18)). With regard to structural and dynamical applications of deuteron NMR, the crucial proposition is that the unique principal direction $\mathbf{e}_Z$ of the QC tensor is, within less than $1°$, parallel to the deuteron's bond direction, $\mathbf{e}_b$. This is rule (ii). Third, if the deuteron is part of a planar structure, e.g., of an aromatic ring, the asymmetry factor η of $\mathbf{Q}$ will substantially deviate from zero. It is then meaningful to consider, apart from $\mathbf{e}_Z$, also the two other principal directions $\mathbf{e}_X$ and $\mathbf{e}_Y$. Adopting the convention $|Q_{ZZ}| > |Q_{XX}| \geq |Q_{YY}|$, rule (iii) states that $\mathbf{e}_X$ is perpendicular to the plane in question. The accuracy of this rule is not as good as that of rule (ii). It appears to be valid within, say, $10°$ (16).

Note that both rules (ii) and (iii) imply that, compared to the QC contributions of the immediate bond, the intermolecular contributions are small, but it is hard to say *how* small they are really.

To verify or falsify rule (ii) for a given compound calls for measuring $\mathbf{e}_Z$ and, independently, $\mathbf{e}_b$ with a precision of better than $1°$. With single crystal NMR it is no serious problem to meet this requirement for $\mathbf{e}_Z$. On the other hand, our experience with X-ray data for $\mathbf{e}_b$ is that the error limits are hardly less than $\pm5°$ even in cases where the published limits are much smaller. Examples of obvious discrepancies of this kind can be found in Refs. (12, 19) and (15, 20). Hence, the only method for getting deuteron bond directions with sufficient accuracy to test rule (ii) meaningfully is neutron diffraction. Still, we are not aware of any case where a nonzero deviation of $\mathbf{e}_b$ and $\mathbf{e}_Z$ outside the combined error limits of the neutron diffraction and NMR experiments has been found (note, we are not talking of deuterons in hydrogen bonds where such deviations have at least been claimed (21, 22)).

Calcium formate is an excellent candidate for testing rules (i)–(iii). From an aquous solution beautiful crystals of the α-form can be grown which show no tendency to weathering even after years in normal atmosphere. The unusual dilution of the deuterons in α-Ca(DCOO)$_2$ and the virtual absence of any other magnetic nuclei lead to exceptionally sharp lines in the deuteron NMR spectra (see below). This allows us to determine the deuteron QC tensors $\mathbf{Q}$ with unprecedented precision. Actually,

as we will see, the final errors of $\mathbf{Q}$ are not dominated by our limited ability to locate the centers of gravity of the resonances. The sharpness of the resonances allows us as well to find the centers of gravity of the quadrupolar split doublets with sufficient accuracy for a measurement of the deuteron CS tensors. The precision achieved exceeds by three times the precision of a former proton line-narrowing multiple-pulse NMR experiment on α-Ca(HCOO)$_2$ (23, 24) which, in terms of the error limits of the obtained CS tensors, is actually the very best such experiment ever performed.

The space group of α-calcium formate is orthorhombic (Pcab) with $Z = 8$ (25), meaning that the spectral information obtainable from rotating only one sample crystal about an axis perpendicular to the applied field $\mathbf{B}_0$ is not only sufficient but already redundant for the measurement of the QC and CS tensors. We will exploit this redundancy to determine within a few hundredths of a degree the direction of the rotation axis of our sample crystal. A careful structure determination of α-Ca(HCOO)$_2$ by neutron diffraction at $T = 100$ K and $T = 296$ K has been performed in 1977 by Burger *et al.* (26) and another by Bargouth and Will in 1981 (27). According to the error limits specified in (26) and (27), the positional parameters in (27) are less accurate by a factor of 2–3 than those in (26). In what follows, we will therefore refer ourselves to the data of Burger *et al.* Figure 1 shows views of the unit cell of α-Ca(HCOO)$_2$ looking down the c and a axes. The asymmetric unit holds two independent formate anions; α-calcium formate thus offers the chance to test rules (i)–(iii) at two distinct deuteron sites.

We will find, for the first time for a carbon-bound deuteron, a deviation of $\mathbf{e}_Z$ from $\mathbf{e}_b$ outside the combined error limits of the NMR and neutron diffraction experiments. We will also find that, for both formate ions, rule (iii) is not valid. It turns out that $\mathbf{e}_Y$, and not $\mathbf{e}_X$, is the principal direction of $\mathbf{Q}$ which is perpendicular to the molecular plane. We will provide a natural reason for this result and, in so doing, also a natural reason for the usual validity of rule (iii).

EXPERIMENTAL

Sample Preparation

The synthesis of Ca(DCOO)$_2$ was started by preparing deuterated formic acid. This was done by repeated exchange of oxalic acid dihydrate, (COOH)$_2 \times 2$H$_2$O, with D$_2$O and drying the product, deuterated oxalic acid, under reduced pressure to get deuterated anhydrous oxalic acid, (COOD)$_2$, followed by thermal decomposition at $160–180°$C to get perdeuterated formic acid, DCOOD. Neutralization with CaCO$_3$ and evaporation to dryness yielded Ca(DCOO)$_2$. Crystals were grown from a saturated solution in H$_2$O at $40°$C (the carbon-bound deuteron of the formate ion does not exchange!) and slow evaporation at the same temperature under constant stirring. Diamond-like crystals of α-Ca(DCOO)$_2$ with diameters of up to 7 mm were obtained after 2 months. Using an optical goniometer, some of
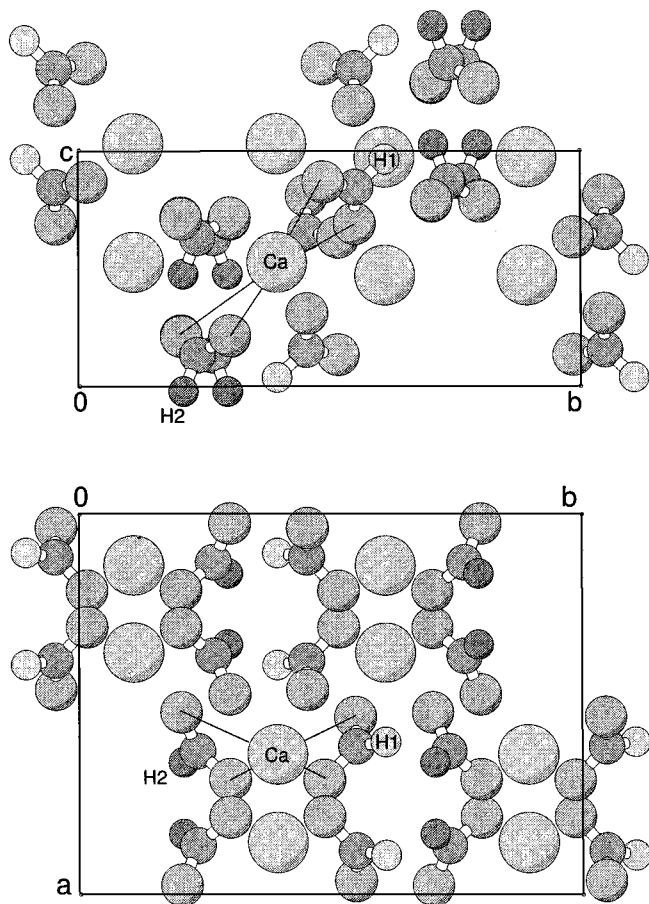
FIG. 1. View of the unit cell of α-Ca(HCOO)$_2$ along a and along c following (26). One of the eight formula units is marked. Pairs of these units are related by inversion centers and are thus magnetically equivalent. Hydrogens of type 1 and type 2 are shaded differently.

the larger of the harvested crystals were examined with regard to the quality of the natural growth planes. A particularly beautiful specimen was selected for NMR. Its natural growth planes were indexed by measuring the angles δ_{pq} between the normals of all pairs of planes p and q and comparing these angles with the angles $\delta_{rs}^{(n)}$ between pairs of low-indexed reciprocal lattice vectors $\mathbf{r}^*$ and $\mathbf{s}^*$ calculated from the neutron diffraction structure data (26). The crystal was fixed with two-component epoxy glue (UHU plus endfest 300, made by UHU GmbH, Bühl, Germany) to a rod made of PVC such that the rod axis (which subsequently was to become the rotation axis of the crystal in the NMR goniometer) had polar angles $\theta \approx 75°$ and $\phi \approx 15°$ in the crystal-fixed axis system $\hat{\mathbf{a}} = \mathbf{a}/a$, $\hat{\mathbf{b}} = \mathbf{b}/b$, $\hat{\mathbf{c}} = \mathbf{c}/c$ where $\mathbf{a}$, $\mathbf{b}$, and $\mathbf{c}$ are the primitive lattice vectors of the orthorhombic cell and $a = 10.168$ Å, $b = 13.407$ Å, and $c = 6.278$ Å (26). The orthorhombic symmetry of the crystal generates effectively three more rotation axes such that rotation of the crystal about the specified axis provides access to much more than the minimum information necessary for measuring the QC and the (symmetric constituent of the) CS tensor. The rod with the crys-

tal was machined on a lathe to a diameter of 4.2 mm, fitting precisely into a standard 5-mm NMR tube cut to an appropriate length (44 mm) for the NMR probe. The rod with the crystal was fixed inside the NMR tube with a droplet of epoxy glue.

Apparatus

With one modification we used the same FT spectrometer that served us in many deuteron NMR studies during the past decade, e.g. (7, 28). It is built around a narrow-bore 11-T Bruker cryomagnet whose driftrate fell over the years well below the 10^{-9}/h level, which is important for the present project. The modification concerns the receiver. The new receiver (29)—christened ADC2000 by our former graduate students because it took a long time to complete it and they knew U.H. would be forced to retire in late 1999—features a local oscillator frequency ν_{loc} for the phase-sensitive detector (mixer) which is lower than the transmitter frequency ν_{tr} ($\approx \nu_L = 72.12$ MHz) by $\nu_{tr}/36 \approx 2$ MHz. This means that an on-resonance deuteron NMR signal appears at the output of the receiver as a (decaying) 2-MHz signal. To prevent noise from the mirror frequency at about 68 MHz to appear, after the mixer, in the 2-MHz band, a steep three-section 72-MHz filter with a flat top of 2-MHz and an attenuation of 26 db at 68 MHz is placed between the preamplifier and the receiver. The 2-MHz signal after the mixer is amplified by an ac amplifier with a virtually flat gain of 20 db from 1 to 3 MHz, dropping to 0 db at 5 MHz and cutting off still higher frequencies. The 2-MHz NMR signal is sampled by a 12-bit, 10-MHz (actually $\nu_{tr} \times 5/36 \approx 10.017$ MHz) analog-to-digital converter. In steps of two, up to 128 K samples can be taken corresponding to a signal duration of 13.1 ms. This was judged sufficient for solid-state deuteron NMR, and as it turned out, it *is* sufficient. Signal accumulation requires that the initial phase of all FIDs to be accumulated is the same. To ensure this requirement, the rise of the RF pulse which excites the FID (or the rise of the pulses which excite an echo) is synchronized to the $\nu_{tr}/36 \approx 2$ MHz signal. Accumulation is under the control of a TMS320C40 signal processor. After completion of the accumulation, this processor performs all necessary steps (including a real Fourier transformation) to generate a phase-corrected spectrum and transfers the interesting part of the spectrum (that centered at 2 MHz and covering a selectable range of, e.g., ± 156.25 MHz) to the host computer for storage on a disc and to a display for visual inspection. The entire software of the signal processor finds room in its cache memory. Therefore, despite the possibly rather long data files (128 K), all computions are performed in a time which is hardly noticeable by the user.

The advantages of the ADC2000 over the former, traditional receiver with quadrature phase detection are as follows:

• The user does not need to care about the amplitude and phase balances of two orthogonal-phase channels. Any phase cycling for counteracting imbalances becomes unnecessary.

• Long-term drifts are excluded because only ac amplifiers are used.

- The receiver contributes virtually nothing to the deadtime of the spectrometer because no narrow video filters are involved that prevent, in traditional designs, "mirror" noise, potentially generated in slowly running ADCs, from being added to the in-band noise. In the ADC2000 no compromises between deadtime and filters are necessary.

- The ADC2000 is tailored to the spurious-signal-suppression scheme described by Speier *et al.* (*28*). It is able to use different file lengths for the signal proper (as mentioned, up to 128 K) and for the spurious signal (e.g., 512 samples), allowing us to reduce the delay between the NMR-saturating, spurious-signal exciting pulses to 2.5 ms. This means that Speier's scheme can be applied to samples with T_1 as short as 10 ms. Using this scheme, an undistorted signal can be recorded not later than 5 μs after the center (which marks the "true" time zero for the FID) of a 2-μs 90° pulse. The remaining dead time is dominated by the bandwidth of the NMR probe.

We should also mention some (minor) disadvantages:

- Because of the synchronization requirements, the programming of the pulse generator (*30*) becomes somewhat more involved, e.g., the spacing of pulses that affect the phase of the NMR signal must be an integer multiple of 500 ns. Other times such as the widths of pulses can remain on the usual 100-ns raster of the pulse generator.

- An on-resonance NMR signal is available as a 2-MHz signal and not as a (decaying) dc signal. This is somewhat inconvenient when adjusting widths of 90° or 180° pulses.

- Because the sampling rate of the ADC is tied to the spectrometer frequency ν_{tr}, the frequency scale of the FT spectra depends slightly on the setting of ν_{tr}. In the data analysis below, this dependence is of course taken into account.

A similar receiver concept is realized in the Avance spectrometers of the Bruker company. In those spectrometers, the sampling rate is, however, substantially smaller than in our ADC2000, and the delicate synchronization problems discussed above are solved in a different way. Also, because of the low sampling rate, quadrature phase detection is still required to avoid mirror noise (*31*).

The spectrometer component that is crucial for the precision of the measurement of QC and CS tensors is the NMR probe and, in particular, its goniometer.

The idea is that the axis **g** of the goniometer is perpendicular to the applied field **B**$_0$. However, we do not know the direction of **B**$_0$. No NMR spectroscopist does. What is available as a reference is the innermost tube of the magnet's cryostat and we can only assume that this tube is parallel to **B**$_0$. The cylindrical NMR probe is 180 mm long and 50 mm in diameter. We wrapped tape around its ends such that the probe fits smoothly but tightly into the cryostat. The drive of the goniometer consists of a worm gear. The bearing of the toothed wheel (which holds the NMR tube with the sample) and that of the NMR tube at the opposite side of the probe—these bearings define the goniometer axis

g—were machined on a milling machine which guarantees orthogonality of probe and goniometer axes within a fraction of a minute of arc. The tolerances of the bearings are such that they keep a possible wobbling of the NMR tube below ±0.03°. The worm of the gear is made of aluminum and the toothed wheel (36 teeth) of Vespel. Both pieces were made many years ago by a firm which specialized in making gears. We expected that their experts would produce a virtually perfect, evenly divided toothed wheel. The NMR results reported below suggest that our expectation was wrong. The worm is connected with a rod of aluminum to a knob and a dial with 100 divisions at the top of the cryostat. When recording spectra for a rotation pattern, we always rotated the knob/worm by one full turn corresponding to a 10° rotation of the sample, and the dial allowed us to set this angle to within ±0.01° (±1/10 division of the dial). Inside the toothed wheel the NMR tube is held by a rubber O-ring which is pressed onto the tube by a hollow screw to prevent any slip between the tube and the wheel. A 100-Ω platinum resistor in the vicinity of the sample served to monitor the temperature.

DATA PROCESSING AND RESULTS

Preparatory Tests

A precision measurement of QC and CS tensors calls for recording NMR spectra for a fairly large number of crystal orientations. In order to find out what the appropriate delay t_w between RF shots is, we first measured the spin–lattice relaxation time T_1. We used the saturation-recovery method and chose more or less arbitrarily the goniometer rotation angle for which **B**$_0$ lies about 5° off the *ab* plane of the crystal. From a series of spectra recorded for a range of delays t_w, we concluded that a certain doublet (actually the innermost) is the slowest to recover, but the others are only marginally faster. T_1 of this doublet was measured and found to be (37 ± 3) min at the temperature $T = (298 \pm 0.5)$ K. The size of T_1 suggests that it is spin diffusion (*32*) which is responsible for the almost uniform relaxation of all distinct deuteron spins in Ca formate. The orthorhombic crystal structure in combination with spin diffusion also suggests that T_1 is only weakly dependent upon the crystal orientation. As a result of this test we decided to choose, for the final tensor measurements, t_w not shorter than 1 h.

Next we tested how many accumulations are needed to obtain spectra with an acceptable signal-to-noise (S/N) ratio. In Fig. 2 we show two spectra. The upper is the Fourier transform of a single FID with the spin system having been in thermal equilibrium at 298 K prior to the 2-μs RF excitation pulse. The lower is an overnight spectrum from 10 accumulated FIDs. In passing, we note that the quality of these spectra should give credit to the performance of the ADC2000. In the single shot spectrum the average width $\delta\nu$ of the lines is 667 Hz, substantially narrower than for "typical" deuterated compounds, and the S/N ranges from 83 to 116, the average being 100. We shall see below that it
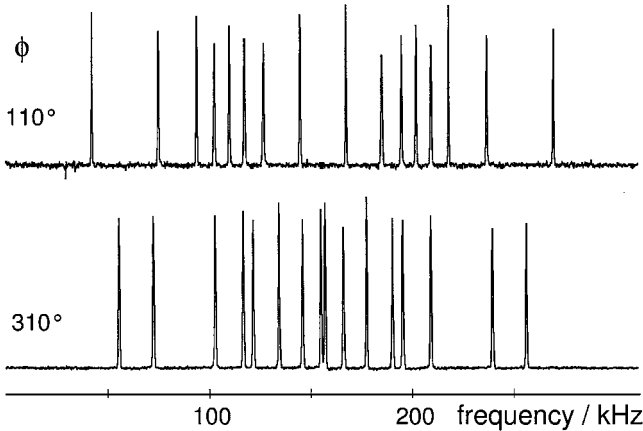
FIG. 2. Deuteron NMR FT spectra of a single crystal of α-Ca(DCOO)$_2$. Top: single-shot spectrum; bottom: overnight spectrum, 10 FIDs accumulated. The rotation angle ϕ refers to Fig. 4. A manual, two-parameter phase correction with a resolution of 1° was applied. From the scatter of the CS data points in Fig. 5 it follows that the centers of gravity of the resonances in these spectra can be located within ±7 Hz. The digital resolution is 152.8484 Hz. The spurious out-of-phase signals on the left end of the single shot spectrum are from an unknown extraneous source. Due to cancellation, they are virtually absent in the overnight spectrum.

is large enough as not to be a limitation to the precision of the QC tensor measurements. By fitting gaussians to the lines we locate their centers of gravity. Theoretically, the standard deviation δ associated with this procedure is (33)

$$\delta = \pm\text{const}\,\delta\nu/(S/N). \quad [1]$$

Extensive numerical tests (14) yielded const = 0.34 ± 0.06. We wondered whether the digital resolution $\delta\nu_{\text{dig}}$ should also show up in [1] and therefore repeated the numerical tests with the same ratio of $\delta\nu/\delta\nu_{\text{dig}}$ as in the actual experiment. These tests confirmed that const ≈ 0.34. By inserting this value in [1] together with $S/N = 100$ and $\delta\nu = 667$ Hz, we get the amazingly small number of ±2.3 Hz for δ.

In FT spectroscopy, however, there is, in addition to noise, another unavoidable source of error in locating the center of gravity of a resonance line. This is the phase-correction step in the data analysis. For that step, we used Heuer's automatic phase-correcting routine (34). Visual inspection of the spectra so obtained conveyed the impression that the phase correction parameters cp and lp (see (34) for their definition) proposed by the routine can still be improved. Therefore, we refined these parameters manually. The quality of the spectra allowed us to find the best values for cp and lp within 1°, and this was also the digital resolution of the manual phase control. In order to learn what the consequence of an erroneous phase correction is, we generated synthetic noisy time data ($S/N = 100$, $\delta\nu \approx 670$ Hz, $\delta\nu/\delta\nu_{\text{dig}} \approx 4.5$, all values as in the experiment), introduced, after Fourier transformation, a phase error of ±1° and determined with the fitting routine the centers of gravity of the lines. The

result of this test was that δ increased from ±2.5 Hz (perfect phase) to ±7.1 Hz (1° phase error) with the sign of δ being correlated, of course, with that of the phase error. Below we will see that the latter number for δ is realistic. It corresponds to only one-hundredth of the linewidth and to only one-twentieth of the digital resolution $\delta\nu_{\text{dig}}$. Essentially the same procedure for locating resonances as used here was adopted in (22). The authors estimate that their precision is about 50 Hz. Looking at the spectra in their Fig. 1 reveals that the phase correction problem was not solved satisfactorily.

The heights of the lines in Fig. 2 differ somewhat from each other. This is caused, on the one hand, by differences of the linewidths $\delta\nu$ and, on the other hand, by the digital resolution which is 152.8484 Hz. Note that the lines of the outermost doublet, whose splitting is 228.4 kHz, are among the highest. This demonstrates the adequacy of both the excitation and the receiving bandwidths of the spectrometer.

Finally, in order to test the mechanical precision of the goniometer and its drive, we compare in Fig. 3 spectra recorded for the rotation angles $\phi = 0°$, 180°, and 360°. If the goniometer, the drive, and the orthogonality of **g** and **B**$_0$ were perfect, the quadrupole splittings $\Delta\nu_Q$ in all of these spectra had to be identical. In the 0° and 360° spectra they indeed agree satisfactorily; in the 180° spectrum, however, they deviate deceivingly much from those in the other two spectra. Actually, for $\phi = 0°$, **B**$_0$ lies close to the bc plane of the crystal and the usually eight distinct doublets become pairwise degenerate. An inspection of the rotation pattern in Fig. 4 (to be discussed below) reveals that doublets 1 and 3 in Fig. 3 (we count them starting from the innermost doublet) are sensitive to a (small) misorientation, while doublets 2 and 4 are insensitive because, for $\phi = 0°$, the path of **B**$_0(\phi)$ either crosses the equator (doublet 2) or passes near the pole (doublet 4) of the respective QC tensor. The splitting $\Delta\nu_Q$ of doublet 1 depends most strongly on ϕ. For this doublet, $\frac{d\Delta\nu_Q}{d\phi}|_{\phi=0°,180°} = 4.16$ kHz/°. The measured splittings of this
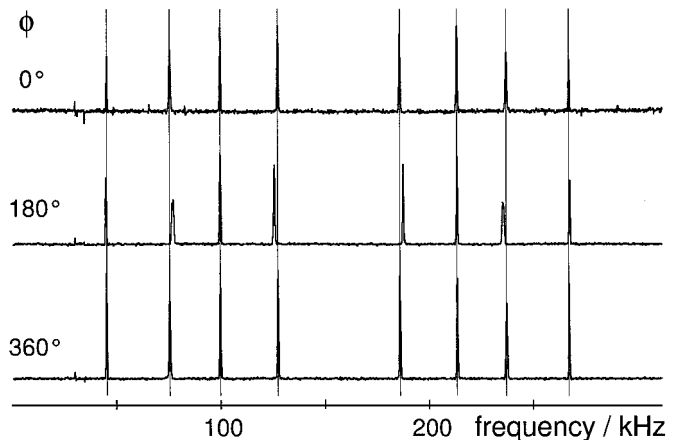
FIG. 3. Test of goniometer settability ($\phi = 0°, 360°$) and of 180°-periodicity ($\phi = 180°$) of the spectra. See text for details and quantitative aspects.
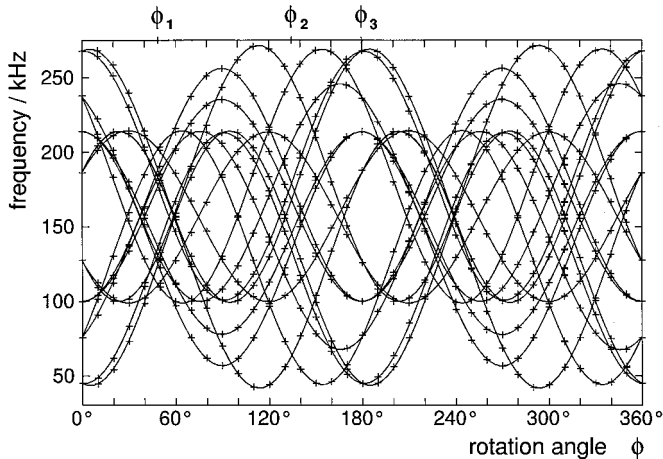
FIG. 4. Rotation pattern of line positions. For $\phi = \phi_1, \phi_2$ and ϕ_3, the applied field is in the ab, ac, and bc plane, respectively. Note the lack of perfect $180°$ periodicity of the pattern. The full curves are fitted harmonic functions (*not* fitted quadrupole splittings). The scatter of the data points relative to the fitted quadrupole splittings plus CSs corresponds to not more than a sixth (!) of the width of the full curves.

doublet in the $0°$ and $360°$ spectra are 58.49 and 58.57 kHz, respectively. That means, after a $360°$ rotation, we reproduced the initial crystal orientation within $0.019°$ which gives credit to the settability of the drive of the goniometer.

On the other hand, the splitting of doublet 1 in the $180°$ spectrum is 61.95 kHz and thus 3.42 kHz larger than, on the average, in the $0°$ and $360°$ spectra. This implies that either the division of the toothed wheel or the orthogonality of $\mathbf{g}$ and $\mathbf{B}_0$, or both, is anything but perfect. As it turns out, the unique axis of one of the two QC tensors contributing to doublet 1 is almost perpendicular to $\mathbf{g}$, meaning that the path of $\mathbf{B}_0(\phi)$ leads from the QC tensor equator right to its pole. This implies that all along that path the splitting $\Delta\nu_Q$ is insensitive to a (small) excursion of $\mathbf{B}_0$ in the perpendicular direction, that is, to a (small) deviation of the angle $\sphericalangle(\mathbf{g}, \mathbf{B}_0)$ from $90°$. Therefore, we must conclude that the major part of the differences in the $\phi = 0°$ and $\phi = 180°$ spectra in Fig. 3 results from an error in the rotation angle ϕ. From the above-quoted numbers it follows that instead of the nominal $\phi = 180°$ rotation, the true rotation angle was only $(180° - 0.82°)$. The splittings of the other doublets in the $180°$ spectrum and the beginning lifting of the degeneracy of the two tensors contributing to doublet 3 support this conclusion, annoying as it is. In the meantime we checked the uniformity of the division of a toothed wheel stemming from the same lot as that in our former deuteron NMR probe (remember, our lab was closed down in late 1999 and all equipment is gone). Using a light pointer and a two-sided mirror fixed to an NMR tube we could confirm that $360°$ rotations are reproducible within less than $0.1°$. On the other hand, $180°$ rotations were consistently in error by roughly $0.3°$. While this toothed wheel is obviously better than the specimen in the NMR probe, the nonuniformity of its division is nevertheless much larger than anticipated.

There is a second QC tensor contributing to doublet 1. Its unique axis is strongly oblique to the goniometer axis $\mathbf{g}$. The splitting of the respective doublet is therefore sensitive to the orthogonality of $\mathbf{g}$ and $\mathbf{B}_0$. The fact that doublet 1 is as sharp in the $180°$ spectrum as it is in the $0°$ spectrum indicates that a possible nonorthogonality of $\mathbf{g}$ and $\mathbf{B}_0$ is not a serious problem.

What to do with the imperfect goniometer? The best solution would obviously be to get a new gear and, after having *verified* that the division of the toothed wheel is uniform, to repeat taking data. Alas, it is too late for that. In Section IV of (*35*) we pointed out that the problem with the unknown angle $\sphericalangle(\mathbf{g}, \mathbf{B}_0)$ can be alleviated by recording rotation patterns of line positions (which are subsequently used for fitting QC and/or CS tensors) over a full turn $0 \leq \phi \leq 2\pi$ and not, as usual, only over the "sufficient" range $0 \leq \phi \leq \pi$. By taking averages $\langle\Delta\nu_Q(\phi)\rangle := \frac{1}{2}[\Delta\nu_Q(\phi) + \Delta\nu_Q(\phi + \pi)]$ and proceeding otherwise as usual, the remaining errors will be kept quadratically small in $\alpha := \sphericalangle(\mathbf{g}, \mathbf{B}_0) - \pi/2$.

We will now argue that exactly the same procedure allows us to cope with a nonuniformly divided goniometer toothed wheel. Denoting the *nominal* rotation angle by ϕ and the *true* rotation angle of the wheel by $\tilde{\phi}$, the nonuniformity can adequately be modeled by

$$\tilde{\phi}(\phi) = \phi + \hat{\varphi}\sin(\phi - \phi_c), \qquad [2]$$

where $\hat{\varphi}$ and ϕ_c are constants whose numerical values we may find by examining pairs of spectra for general values of ϕ and $\phi + 180°$, and not only those for $\phi = 0°$ and $\phi = 180°$ as we did so far. In this way we got $\hat{\varphi} = 0.01 \cong 0.6°$ and $\phi_c = 60°$. For any nominal angle ϕ we might now calculate a correction $\Delta\phi = \tilde{\phi}(\phi) - \phi$ and take this correction into account in the tensor fitting procedure. Alternatively, we may calculate from the raw data $\Delta\nu_Q^{raw}(\phi)$ corrected quadrupole splittings

$$\Delta\nu_Q^{corr}(\phi) = \Delta\nu_Q^{raw}(\phi) - \frac{d\Delta\nu_Q(\phi)}{d\phi}\Delta\phi, \qquad [3]$$

where, because $\Delta\nu_Q(\phi) = A + B\cos 2(\phi - \phi_0)$ with A, B, and ϕ_0 being constants,

$$d\Delta\nu_Q(\phi)/d\phi = -2B\sin 2(\phi - \phi_0). \qquad [4]$$

Equations [2]–[4] imply that $\Delta\nu_Q^{corr}(\phi) - \Delta\nu_Q^{raw}(\phi)$ is equal in magnitude and opposite in sign for ϕ and $\phi + 180°$. Therefore, within the validity of [2] and the linear approximation [3], the averages $\langle\Delta\nu_Q^{corr}(\phi)\rangle$ and $\langle\Delta\nu_Q^{raw}(\phi)\rangle$ are equal. Hence, by taking such averages we may forget about the difference of raw and corrected quadrupole splittings, or nominal and true rotation angles. In this way all errors are eliminated which are linear not only in α, but also in $\hat{\varphi}$. Below, we will adopt this procedure. The remaining errors are of order $\hat{\varphi}^2$ and α^2. For $\hat{\varphi} = 0.01$, the worst case error will be, in terms of the quadrupole splitting, $2\hat{\varphi}^2 C_Q \approx 33$ Hz. This (systematic) error is larger than the

standard deviation of locating line positions, but smaller than the error stemming from the uncertainty of setting the goniometer dial. Nevertheless, it contributes significantly to the final measurement error of the QC tensors. Due to the smallness of the deuterons' CS anisotropies, the imperfection of the goniometer has no consequences for the precision of the measurement of the CS tensors.

Rotation Pattern of Line Positions and Data Analysis; Quadrupole Coupling Tensors

From our sample crystal of α-Ca(DCOO)$_2$ we recorded deuteron spectra for $\phi_n = n \times 10°, n = 0, \ldots, 36$. During daytime we chose $t_w = 1$ h and recorded single shot spectra. Overnight, 10 FIDs were accumulated. The sample temperature was not regulated but monitored and found to be $T = (287 \pm 0.5)$ K during all the time of data taking. After baseline (36) and phase correcting the spectra, the centers of gravity of all resonances were located as described above and written in a file. From this file, the rotation pattern shown in Fig. 4 was generated. In order to find out which resonances arise from the same nuclei in subsequent spectra, we fitted sin-curves to the data points. These sin-curves are also shown in Fig. 4. In the range $0° \le \phi \le 180°$ there are three angles $\phi_1 = 48.57°$, $\phi_2 = 134.41°$, and $\phi_3 = 179.67°$ (the digits behind the decimal point are obtained by a fitting procedure, see below) where all the sin-curves cross pairwise. At these angles the path $\mathbf{B}_0(\phi)$ crosses the *ab*, *ac*, and *bc* planes, respectively, of the orthorhombic crystal. By looking at *which pairs* of sin-curves cross at ϕ_1, ϕ_2, and ϕ_3, we can partition these curves in two sets which we label, for convenience, as *red* and *blue* sets. Eventually, these sets must be assigned to the two types of distinct deuterons in the crystal; see below.

The crossing points ϕ_1, ϕ_2, and ϕ_3 play an additional role in the data analysis: Above we stated that because of the orthorhombic symmetry of α-Ca(DCOO)$_2$ one rotation pattern with doublets from four symmetry related deuterons is worth four rotation patterns for one deuteron. The four rotation axes are generated from the original one with polar angles $\vartheta_R \approx 75°$, $\varphi_R \approx 15°$ by twofold rotations about the primitive axes of the crystal which are all parallel to 2_1 axes. We are free to assign any one pair of sin-curves (corresponding to some doublet in the spectrum) from, say, the red set, to the original rotation axis. After that, there is no freedom left. By looking at which individual sin-curves cross at ϕ_1, ϕ_2, and ϕ_3, respectively, we may find out to which of the rotated rotation axes the other sin-curves must be assigned. For example, the sin-curve which crosses that assigned to the original rotation axis at ϕ_1, i.e., where $\mathbf{B}_0(\phi)$ is in the *ab* plane, must be assigned to the rotation axis generated from the original one by a $180°$ rotation about the **c** axis.

After having decided which of the data points in Fig. 4 belong to the red and which to the blue set, and which sin-curves go with which rotation axis, we evaluated the splittings $\Delta\nu_Q^{(d)}(\phi_n)$ ($d = 1, \ldots, 8$ labels the doublets) as well as the centers of

gravity $\nu_{cg}^{(d)}(\phi_n)$ of all doublets. As suggested by the discussion above, we then took the averages

$$\langle \Delta\nu_Q^{(d)}(\phi_n) \rangle := \frac{1}{2}\big[\Delta\nu_Q^{(d)}(\phi_n) + \Delta\nu_Q^{(d)}(\phi_n + 180°)\big]$$

and

$$\langle \nu_{cg}^{(d)}(\phi_n) \rangle := \frac{1}{2}\big[\nu_{cg}^{(d)}(\phi_n) + \nu_{cg}^{(d)}(\phi_n + 180°)\big].$$

Next, the red set of averages $\langle \Delta\nu_Q^{(d)}(\phi_n) \rangle$ was subjected to the tensor fitting program SUPERFIT. The original (Fortran) version of this program was brought in 1979 to the MPI in Heidelberg by J. Tegenfeldt from Uppsala. Since then it was updated several times and is now used in a C^{++} version.[1] One of us (U. H.) discussed it at NMR schools in Waterloo (1991) and Portoroz (1993) and even prepared lecture notes. SUPERFIT is much more versatile and flexible than the still often advertised Volkoff method (37) which stipulates that quadrupole splitting or chemical shift rotation patterns from three mutually orthogonal rotation axes have been recorded. The ability of SUPERFIT to accept data from an arbitrary set of orientations $\Omega^{(B)} := (\vartheta^{(B)}, \varphi^{(B)})$ of $\mathbf{B}_0$ is essential to this work. SUPERFIT provides a least-squares fit of $n = 1, 2, \ldots, N \ge 5$ measured quadrupole splittings $\Delta\nu_{Q,n}(\Omega_n^{(B)})$ or of $n = 1, 2, \ldots, N \ge 6$ chemical shifts $(\nu_n(\Omega_n^{(B)}) - \nu_L)/\nu_L$ to a traceless QC tensor $\mathbf{Q}$, or a general symmetric second-rank tensor σ. In the fitting procedure, the orientations $\Omega_n^{(B)}$ of $\mathbf{B}_0$ are assumed to be known exactly—which, of course, is not the case. The tensors are specified by their cartesian components $Q_{\alpha\beta}$ and $\sigma_{\alpha\beta}$ in a crystal-fixed, but otherwise arbitrary orthogonal axes system Σ to which $\vartheta^{(B)}$ and $\varphi^{(B)}$ are also referenced. For α-Ca(DCOO)$_2$ it is natural to choose the axes of Σ along **a**, **b**, and **c**. Because the measured quantities $\Delta\nu_{Q,n}$ and ν_n are linear functions of the $Q_{\alpha\beta}$ and $\sigma_{\alpha\beta}$, respectively, least-squares fitting is a noniterative process. Note that least-squares fitting of second-rank tensors becomes a cumbersome iterative process with the need of guessing starting values if the tensor is specified by its principal values and the Euler angles relating its principal directions to the axes of the reference frame, see, e.g., (38).

The following feature of SUPERFIT assists in handling data from rotation patterns and is useful for finding refined orientations of $\mathbf{B}_0$: Instead of specifying $\Omega_n^{(B)}$ for each measurement n, the direction ϑ_R, φ_R of the crystal's rotation axis, a reference direction $\vartheta_{ref}, \varphi_{ref}$, and a reference angle ϕ_{ref} are given together with the rotation angle ϕ_n. For $\phi = \phi_{ref}$, $\mathbf{B}_0(\phi)$ is parallel to the projection of the reference direction onto the plane perpendicular to the rotation axis. From $\vartheta_R, \varphi_R, \vartheta_{ref}, \varphi_{ref}, \phi_{ref}$, and ϕ_n SUPERFIT calculates $\vartheta_n^{(B)}$ and $\varphi_n^{(B)}$. For all data of a rotation

---

[1] The source code of SUPERFIT is available on request. Contact Heike Schmitt; e-mail: heike@mpimf-heidelberg.mpg.de.

pattern, the angles $\vartheta_R, \ldots, \phi_{ref}$ are fixed parameters and only ϕ_n varies. In this work we chose as the reference direction the crossing of the path $\mathbf{B}_0(\phi)$ with the ac plane. This choice links the reference direction to the direction of the rotation axis, namely $\vartheta_{ref} = \tan^{-1}(1/\tan\vartheta_R \cos\varphi_R)$ and $\varphi_{ref} = 180°$ and says that ϕ_{ref} equals ϕ_2. Note that the specification of the reference direction does not introduce any extra uncertainty. On the other hand, our way of preparing the sample crystal left some uncertainty in ϑ_R, φ_R and ϕ_{ref}. Therefore, we refined these angles by minimizing for the red data set of quadrupole splittings the standard deviation $\sigma = \{\sum_{n=1}^{N}(\Delta\nu_{Q,n} - \Delta\nu_{Q,n}^{fitted})^2/(N-5)\}^{1/2}$, which is also provided by SUPERFIT, with respect to ϑ_R, φ_R and ϕ_{ref}. It turned out that σ_{red} is sensitive to changes of ϕ_{ref} down to 0.001° and to changes of ϑ_R and φ_R down to 0.01°. During the minimization process we identified a few data points as outliers and discarded them. In each such case we verified that there is a plausible reason for the qualification as "outlier," e.g., overlapping of lines.

The refinement led to $\vartheta_R = 75.40°$, $\varphi_R = 16.12°$, and $\phi_{ref} = 134.407°$ and brought σ_{red} down to 83 Hz. In passing we mention that it was by using these values of ϑ_R, φ_R and ϕ_{ref} that further up we obtained the digits behind the decimal point of ϕ_1, ϕ_2, and ϕ_3.

There is a natural way to check the reliability of these numbers: The fitting procedure may be repeated for the blue data set and the question is whether it converges to the same values of ϑ_R, φ_R and ϕ_{ref}. When we did it we were greatly relieved to find that the minimum of σ_{blue} occured within 0.02° for the same values of ϑ_R and φ_R and within 0.005° of the same value of ϕ_{ref} as did that of σ_{red}. The minimum value of σ_{blue} turned out to be 97 Hz.

In Table 1 we list the red and blue QC tensors as they are obtained after the refinement. Below it will turn out that the blue tensor (the red tensor) must be assigned to one of the four symmetry related deuterons of type 1 (of type 2) of the crystal. This labeling of the deuterons follows (*26*). For convenience, we list the tensors both in their cartesian form and by their principal values and principal directions. The QC tensors of the other deuterons in α-Ca(DCOO)$_2$ are obtained from those in Table 1 by inverting in the cartesian tensor forms the sign of any two of the off-diagonal elements Q_{xy}, Q_{xz}, and Q_{yz}, while keeping the third and all diagonal elements unchanged.

The Chemical Shift Tensors

The center of gravity $\langle\nu_{cg}^{(d)}(\phi_n)\rangle$ of a doublet d reflects the (negative) chemical shift $\nu_L \cdot \mathbf{B}_0/B_0 \cdot \boldsymbol{\sigma}^{(d)} \cdot \mathbf{B}_0/B_0$ plus the second-order quadrupolar shift $S^{(d)}(\phi_n)$ of a deuteron d. The partition of these shifts into red and blue sets and their assignment to one of the four rotation axes follows immediately from the analysis of the quadrupole splittings $\langle\Delta\nu_Q^{(d)}(\phi_n)\rangle$. Because we know the tensors $\mathbf{Q}^{(d)}$, we may compute the shifts $S^{(d)}(\phi_n)$. For axially symmetric tensors $\mathbf{Q}$ (*39*),

$$S(\phi_n) = \frac{Q_{ZZ}^2}{24\nu_L}\left[1 - \left(\frac{\Delta\nu_Q(\phi_n)}{Q_{ZZ}}\right)^2\right]. \qquad [5]$$

$S(\phi_n)$ is maximal for $\Delta\nu_Q = 0$. For α-Ca(DCOO)$_2$ and $\nu_L = 72.12$ MHz, the maximum of S/ν_L is 0.42 ppm. Because the second-order quadrupole shifts are less-than-10% corrections of the chemical shifts and because the asymmetry parameters η of both the red and the blue $\mathbf{Q}$ tensors are small (see Table 1), Eq. [5] is here a perfectly valid approximation. In Fig. 5 we display the pure chemical shifts $\{[\langle\nu_{cg}^{(d)}(\phi_n)\rangle - \nu_L] - S^{(d)}(\phi_n)\}/\nu_L$ vs ϕ. The chemical shift tensors obtained by subjecting these data to SUPERFIT are listed in Table 2. The sin-curves in Fig. 5 correspond to the fitted tensors.

TABLE 1
The Deuteron QC Tensors in α-Ca(DCOO)$_2$

Site 1	Principal value (kHz)	Principal direction (ϑ, φ)
$\mathbf{Q}_{blue}/\text{kHz} = \begin{pmatrix} -110.13 & -20.93 & -22.30 \\ -20.93 & 65.60 & 168.75 \\ -22.30 & 168.75 & 44.53 \end{pmatrix}$	$Q_{XX} = -115.45$ $Q_{YY} = -111.46$ $Q_{ZZ} = 226.91$	$\mathbf{e}_X = (51.7°, 319.6°)$ $\mathbf{e}_Y = (112.8°, 30.2°)$ $\mathbf{e}_Z = (46.98°, 97.09°)$
Asymmetry factor $\eta = 0.018$ Standard deviation $\sigma = 0.097$ kHz		

Site 2	Principal value (kHz)	Principal direction (ϑ, φ)
$\mathbf{Q}_{red}/\text{kHz} = \begin{pmatrix} -88.62 & 36.04 & -85.99 \\ 36.04 & -70.76 & -110.67 \\ -85.99 & -110.67 & 159.38 \end{pmatrix}$	$Q_{XX} = -116.84$ $Q_{YY} = -114.30$ $Q_{ZZ} = 231.14$	$\mathbf{e}_X = (92.3°, 317.6°)$ $\mathbf{e}_Y = (63.0°, 46.4°)$ $\mathbf{e}_Z = (27.11°, 232.11°)$
Asymmetry factor $\eta = 0.011$ Standard deviation $\sigma = 0.083$ kHz		

Note. For convenience, both the cartesian and the principal component/principal direction representations are given. Both are referenced to the $\hat{\mathbf{a}}$, $\hat{\mathbf{b}}$, $\hat{\mathbf{c}}$ frame. The uncertainty of $\mathbf{e}_Z$ is 0.035°; that of $\mathbf{e}_X$ and $\mathbf{e}_Y$ is 1°.

TABLE 2
Principal Values and Principal Directions of the Traceless Part of the Deuteron/Proton Chemical Shift Tensors in α-Ca(HCOO)$_2$

Site	Principal values (ppm)		Principal directions[a] (ϑ, φ)	
	This work	Ref. (24)	This work	Ref. (24)
1	3.18 ± 0.06[b]	3.1 ± 0.2	52.3°, 104.6°	53°, 105°
(blue)	0.06 ± 0.06	0.2 ± 0.2	49.6°, 333.3°	52°, 340°
	-3.24 ± 0.06	-3.3 ± 0.2	116.9°, 37.7°	121°, 42°
2	2.58 ± 0.06	2.7 ± 0.2	92.7°, 316.2°	93°, 319°
(red)	0.88 ± 0.06	0.7 ± 0.2	158.8°, 53.1°	158°, 56°
	-3.46 ± 0.06	-3.4 ± 0.2	69.0°, 45.2°	68°, 48°

Note. Difference of isotropic shifts $\sigma_{\text{iso,blue}} - \sigma_{\text{iso,red}} = 0.33$ ppm (this work), 0.23 ppm (Ref. (24)).

[a] Polar angles in the $\hat{\mathbf{a}}, \hat{\mathbf{b}}, \hat{\mathbf{c}}$ frame.
[b] Statistical error.
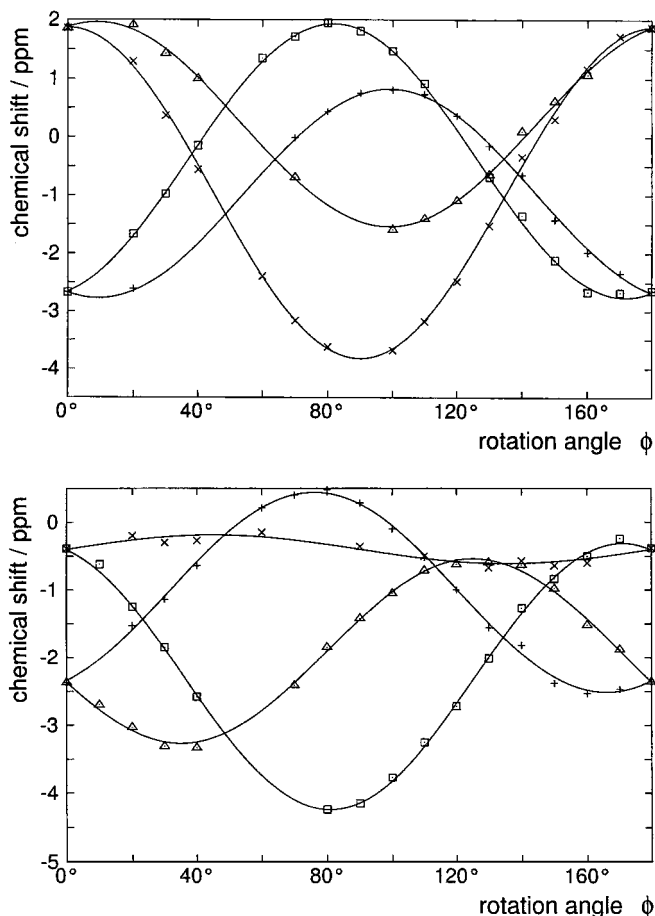
FIG. 5. Chemical shifts $[\langle \nu_{\text{cg}}(\phi) \rangle - \nu_{\text{L}} - S(\phi)]/\nu_{\text{L}}$ vs the rotation angle ϕ. Top: blue data set; bottom, red data set. The full curves correspond to the fitted CS tensors. The scatter of the data points relative to these curves indicates that resonances in the spectra could be located with an uncertainty of ± 7 Hz.

DISCUSSION

Error Considerations

The standard deviation σ of the measured chemical shifts from the best fit curves is 0.057 ppm corresponding to 4.1 Hz. This number is also a conservative estimate of the statistical uncertainty of both the cartesian and the principal components of the CS tensors. The estimate is conservative because of the large redundancy of the experimental data.

Provided that σ is dominated by the uncertainty of the phase correction and by the noise, we expect for σ a value of $\frac{1}{2} \cdot 7.1$ Hz = 3.55 Hz (remember, $\langle \nu_{\text{cg}}(\phi_n) \rangle$ results from averaging *four* individual line positions). The close matching of the expectation with the actual standard deviation means that we have not overlooked other significant sources of statistical errors and that certain types of potential systematic errors including the drift of $\mathbf{B}_0$ are negligible. The bulk magnetic susceptibility of the sample is another potential source of systematic errors. It is not excluded by the argument we just put forward. It has two aspects. The first concerns the shift of the NMR line when, as viewed along $\mathbf{B}_0$, the shape of the sample changes (remember, the sample is rotated). This shift scales with the isotropic part χ_{iso} of the sample's volume susceptibility χ. For Ca-formate, $\chi_{\text{iso}} = 0.613$ ppm (40). This problem is essentially eliminated by shaping the sample crystal, as we did, into cylindrical form. What remains are shifts resulting *from* and proportional *to* the anisotropy $\Delta \chi$ of χ. For Ca-formate, $\Delta \chi$ is not known, but from the rather uniform distribution of the Ca ions, and from the zigzag arrangement of the Ca(HCOO)$_2$ units in the primitive cell (see Fig. 1), it may safely be concluded that $\Delta \chi$ is substantially smaller than χ_{iso}. Shifts caused by $\Delta \chi$ can be avoided altogether by working with a spherical sample. For cylindrical samples the shifts are minimal if the length/diameter ratio of the sample is equal to 1, which for our sample was the case at least approximately. Although a quantitative estimate of the influence of χ on the measured CS tensors remains difficult, we are confident that it does not exceed 0.1 ppm.

The average standard deviation of 90 Hz of the measured doublet splittings from the simulated best fit curves is also a valid estimate of the error limits of the cartesian and principal components of the QC tensors. These limits include statistical as well as systematic errors. Remaining systematic errors revealed themselves by the fact that in the process of refining the direction $\vartheta_{\text{R}}, \varphi_{\text{R}}$ of the sample's rotation axis the scattering of the measured splittings around the best fit curves did not become perfectly random. The dominating statistical and systematic errors result, unlike those of the chemical shifts, from the errors of the goniometer setting and from the nonuniformly divided toothed wheel. The size of these errors conforms with the estimates given under Experimental.

Treating, as we did implicitly, the quadrupolar Hamiltonian $\mathcal{H}_Q$ by first-order perturbation theory is adequate because the doublet *splittings* are insensitive to second-order shifts, which

do not exceed 30 Hz (see above), and because third-order terms, which do affect the doublet splittings, will be smaller than that value by roughly a factor of $Q_{ZZ}/\nu_L \approx 0.003$.

The uncertainty of 90 Hz of the off-diagonal elements of $\mathbf{Q}$ corresponds to an uncertainty of $0.015°$ of the unique QC tensor direction. Adding to this number the uncertainty of $0.02°$ in the determination of the direction of the sample's rotation axis (see above) leads us to claim that we have measured the unique QC tensor directions at the sites of the deuterons in α-Ca(DCOO)$_2$ with an uncertainty of not more than $0.035°$.

The Quadrupole Coupling Tensors

We begin by comparing the principal directions $\mathbf{e}_{Zblue}$ and $\mathbf{e}_{Zred}$ from Table 1 with the C–D bond directions $\hat{\mathbf{b}}_1 = (\vartheta_{b1}, \varphi_{b1})$ and $\hat{\mathbf{b}}_2 = (\vartheta_{b2}, \varphi_{b2})$. From the positional parameters in (26) we deduce $\hat{\mathbf{b}}_1 = (46.65°, 98.67°)$ and $\hat{\mathbf{b}}_2 = (26.49°, 231.50°)$, and $\delta_1 = \sphericalangle(\mathbf{b}_1, \mathbf{e}_{Zblue} = 1.21°$ and $\delta_2 = \sphericalangle(\mathbf{b}_2, \mathbf{e}_{Zred} = 0.68°$. It is this result that leads us to assign $\mathbf{Q}_{blue}$ to a deuteron of type 1 and $\mathbf{Q}_{red}$ to a deuteron of type 2. We wish to point out that for this presentation we selected, of course, one of the deuterons of type 1 and one of type 2 such that closely matching pairs of bond and unique QC tensor directions are obtained.

As we can be confident that $\mathbf{e}_{Zblue}$ and $\mathbf{e}_{Zred}$ are reliable within $\pm 0.035°(=: \sigma_{NMR})$, it depends on the precision of the neutron scattering data whether we can claim to have detected deviations of unique QC and C–D bond directions. From the error limits specified in (26) for the carbon and hydrogen positional parameters (296 K data set), we deduce a standard deviation $\sigma_n = 0.28°$ for both $\mathbf{b}_1$ and $\mathbf{b}_2$. We thus conclude that with a $4(\sigma_n + \sigma_{NMR})$ confidence there *is* a deviation δ_1 between the direction of the carbon–hydrogen bond $\mathbf{b}_1$ and the unique principal direction $\mathbf{e}_{Zblue}$ of the QC tensor of deuteron 1. This result hinges critically on the reliability of the stated error limits in (26). Therefore, we have taken the first steps to convince the project selection committee of the ILL in Grenoble, France, that a neutron diffraction reexamination of the structure of α-Ca-formate, taking advantage of the availability of perdeuterated crystals, would be a worthwhile project. For deuteron 2 and bond $\mathbf{b}_2$, the deviation δ_2 amounts to only $2(\sigma_n + \sigma_{NMR})$ and we cannot say that this is a significant difference from zero.

To put the deviations δ_1 and δ_2 in perspective, we note that the direction $\mathbf{b}_1$ following (26) differs from that following (27) by $0.87°$. For $\mathbf{b}_2$, the difference is as much as $1.52°$. That means carbon–hydrogen bond directions deduced from two independent neutron diffraction data sets can deviate from each other as much, in fact even more, than bond and unique QC tensor directions. On the other hand, as the error limits cited by Bargouth and Will imply $\sigma_n = 0.70°$ for both $\hat{\mathbf{b}}_1$ and $\hat{\mathbf{b}}_2$, the above-quoted discrepancies between the two neutron structure investigations are within one (combined) standard deviation for $\mathbf{b}_1$ and within two standard deviations for $\mathbf{b}_2$, and are thus no reason for worrying but rather give credit to the error estimates of the authors.

The deviation δ_1 of $\mathbf{e}_{Zblue}$ from $\mathbf{b}_1$ has about equal components parallel ($\delta_{1\parallel}$) and perpendicular ($\delta_{1\perp}$) to the plane of the formate ion which is very nearly flat (26). While the in-plane component ($\delta_{1\parallel}) \approx 0.8°$ may result from unequal charges on the oxygens of the formate ion, the out-of-plane component ($\delta_{1\perp}) \approx 0.8°$ must have its origin in interionic QC contributions. In the principal axes system of the intraionic QC tensor, it takes an off-diagonal element of $\mathbf{Q}_{interionic}$ of roughly 4.8 kHz to push $\mathbf{e}_Z$ away by $0.8°$ from the plane of the formate ion. We thus conclude that this number (4.8 kHz) reflects the scale of the interionic contributions to the deuteron QC tensors in Ca-formate. By considering the difference $Q_{ZZred} - Q_{ZZblue} = 4.2$ kHz and assigning it exclusively to interionic QC contributions, we arrive at the same result. Unlike the argument based on $\delta_{1\perp}$, this result is, however, not perfectly conclusive because a small difference of the bond lengths b_1 and b_2, which is well compatible with the error limits of (26), can also be responsible for the observed difference of Q_{ZZred} and Q_{ZZblue}.

The asymmetry η of both $\mathbf{Q}_{red}$ and $\mathbf{Q}_{blue}$ must be classified as *small*. Nevertheless, the precision achieved in this work gives meaning to the principal directions $\mathbf{e}_X$ and $\mathbf{e}_Y$ and to the difference between the "equatorial" principal components Q_{XX} and Q_{YY}. Most important, of both $\mathbf{Q}_{red}$ and $\mathbf{Q}_{blue}$ it is $\mathbf{e}_Y$, and not $\mathbf{e}_X$ as predicted by rule (iii), which is close to the normal $\mathbf{n}$ of the respective molecular plane, $\sphericalangle(\mathbf{n}_1, \mathbf{e}_{Yblue}) = 13.8°$, $\sphericalangle(\mathbf{n}_2, \mathbf{e}_{Yred}) = 7.5°$. Why is Ca-formate (and likewise cupric formate (41) and strontium formate (42), but not formic acid (43)) an exception to rule (iii)? The reason is, as we will argue now, the negative charge on the oxygens of the formate ion.

From an extensive molecular orbital study of the EFG at the various deuteron sites in glycine, Davidson *et al.* (44) concluded that a point charge model (p.ch.m.) should be adequate to account for the direct intermolecular EFG contributions at the sites of deuterons. However, there is also a polarization effect whose size is difficult to predict but can be, for deuterons in hydrogen bonds, three times as large as the direct effect. For deuterons bound to carbons, it is claimed to be significantly smaller (44). Despite all reservations, we will now consider the EFG contribution from the charge on the oxygens at the deuteron site in the formate ion also as an *inter*molecular contribution and apply the p.ch.m. A set of point charges q_i, $i = 1, 2, 3, \dots$, at positions $\mathbf{r}_i = (x_i, y_i, z_i)$ produces at the site $\mathbf{r}_k = (x_k, y_k, z_k)$ of a test nucleus k an electric field gradient $\mathbf{V}$ with components

$$V_{\alpha\beta} = \frac{e}{4\pi\varepsilon_0} \sum_i (q_i/e) \frac{3(\alpha_k - \alpha_i)(\beta_k - \beta_i) - (|\mathbf{r}_k - \mathbf{r}_i|)^2 \delta_{\alpha\beta}}{(|\mathbf{r}_k - \mathbf{r}_i|)^5},$$

[6]

where ε_0 is the permittivity of free space and $\alpha, \beta = x, y, z$. As $\mathbf{Q} = \frac{3}{2}(eQ/h)\mathbf{V}$, $Q_{\alpha\beta}$ is expressed by the same sum as in [6] with a prefactor of 149.37 kHz if distances are measured in angstroms. The most critical part in applications of the p.ch.m. is the choice of the charges q_i/e. Here we follow,

very naively, a sophomore's guess:[2] Only the Ca ions and the oxygens bear charges, $q_{Ca}/e = +2$ and, as the crystal must be neutral, $q_O/e = -1/2$. From the oxygens of the formate ion which contains the test deuteron, Eq. [6] then predicts (averaged over both ions) a contribution $\mathbf{Q}_{oxygen}$ with principal components -20.6, 18.8, and 1.8 kHz and principal directions, in the same order, along the bond $\mathbf{b}$, along the normal $\mathbf{n}$, and perpendicular to $\mathbf{b}$ and $\mathbf{n}$. If $\mathbf{Q}_{oxygen}$ is added to a dominant tensor which is axially symmetric along $\mathbf{b}$, we get a resulting tensor $\mathbf{Q}$ which indeed reflects the experimental observation that it is $\mathbf{e}_Y$ which is close to $\mathbf{n}$. However, the calculated value of 17 kHz for the difference $Q_{YY} - Q_{XX} = \eta Q_{ZZ}$ is much larger than in the experiment where it is 4.0 and 2.5 kHz for the blue and red tensors, respectively. Does this mean that the p.ch.m. with $q_O/e = -1/2$ grossly overestimates the EFG contributions from the oxygens?

Not necessarily. The reason for the discrepancy between calculated and observed values of ηQ_{ZZ} may well be the assumption that the dominant part of the EFG is axially symmetric along the bond. The carbon atom in the formate ion is sp^2 hybridized as it is in many molecules with pronounced molecular planes. Examples of such molecules, for which the deuteron QC tensors have been measured, are anthracene (*10*), pyromellitic acid (*12*), dimethylterephthalic acid (*45*), acetylsalicylic acid, also called aspirin (*45*), bullvalene (*16*), fluorene (*17*), azulene (*46*), potassium hydrogen maleate (*47*), and, as already mentioned, formic acid (*43*). All these tensors $\mathbf{Q}$, a total of 24, obey rule (iii). Indeed, an electron in a p_z orbital, with a compensating positive charge at the origin, produces at a nuclear site in the plane perpendicular to the orbital an EFG whose component along the z axis of the orbital is larger in magnitude than that which is perpendicular to the bond and the orbital. This is exactly what rule (iii) states. Elementary as this explanation for rule (iii) is, it seems that it has never been put forward in print. In the compounds listed above, the difference $|Q_{XX}| - |Q_{YY}|$ ranges from 5.2 (aspirin, position D$_2$) to 20.4 kHz (bullvalene, position 3B), the average is about 13 kHz.

In the formate ion, both effects discussed in the previous two paragraphs are present. They lead to opposite differences of the equatorial principal components of $\mathbf{Q}$, which almost cancel each other. This is the reason why the measured asymmetry factors η in α-Ca-formate are so small; see Table 1. In the light of this discussion it even appears as fortuitous that the charge-on-the-oxygens effect wins against the nearby-p_z-orbital effect. Indeed we cannot exclude for sure that the violation of rule (iii) in α-Ca(DCOO)$_2$ results from intermolecular EFG contributions. The

fact that both $\mathbf{Q}_{red}$ and $\mathbf{Q}_{blue}$ violate rule (iii), as do the $\mathbf{Q}$ tensors in cupric and strontium formate, speaks, however, against this possibility.

Finally, we point out that the deuteron QC constants $C_Q = e^2qQ/h(=\frac{2}{3}Q_{ZZ})$ in Ca-formate are unusually small, $C_{Qred} = (154.09 \pm 0.06)$ kHz, $C_{Qblue} = (151.27 \pm 0.06)$ kHz. For the deuterons bound to the sp^2 carbons listed further up, C_Q ranges from 168.4 (pyromellitic acid) to 182.2 kHz (azulene); the average is 178.2 kHz. Small values of C_Q were also reported for formic acid and for cupric and strontium formate (cf. Table 2 in (*47*)), but Ca-formate is extreme. As an explanation, two reasons come to mind. First, formic acid and the formate ion are light units, lighter than all the molecules with sp^2 carbons listed further up, and hence prone to large-amplitude librations. Such librations reduce the time-average EFG which is accessed in an experiment. A test of this proposition is measuring C_Q as a function of the temperature T. This is what Soda and Chiba did for cupric formate (*41*). Lowering T from 291 to 153 K led to an increase of C_Q from (155.3 ± 2.5) to 161 kHz, and an extrapolation to $T \to 0$ K led to the conclusion that in a perfectly static lattice C_Q would be 166 kHz. This is still an unusually small value for a deuteron bound to a carbon. Therefore, the following second reason should also be taken into consideration: Above we argued that the nearby-p_z-orbital and the charge-on-the-oxygen effect nearly cancel each other with regard to the EFG components perpendicular to the C–D bond. By contrast, they strengthen each other with regard to the component parallel to the bond, that is, with regard to C_Q. Both effects tend to lower C_Q and this tendency is the stronger the more charge there is on the oxygens.

The Chemical Shift Tensors

As mentioned in the Introduction, Post measured in 1978 the proton CS tensors in α-Ca(HCOO)$_2$ by line-narrowing multiple-pulse NMR (*23, 24*). In that work, the assignment of the measured CS tensors to the eight magnetically inequivalent proton sites in the unit cell turned out to be a tremendously hard problem and the assignment which Post eventually proposed on the basis of several weak observational and additional intuitive arguments was anything but certain, cf. (*24*, p. 24, end of second paragraph). Note that in the present work the assignment is perfectly safe. We are glad that we can now confirm that Post's assignment is correct. In Table 2 we included his results in terms of the principal components (estimated error limits ± 0.2 ppm) and principal directions of the traceless part of the CS tensors. It is very satisfying that for all six principal components the difference of the former and the present result (which is three times more precise) is indeed smaller than ± 0.2 ppm. Likewise, the principal directions agree within the expected error limits. Because the present deuteron NMR study fully confirms Post's proton NMR results, his discussion of the CS tensors in α-Ca(HCOO)$_2$ is still valid and we can restrict ourselves here to a few remarks.

---

[2] This guess leads, actually, to severe problems if we attempt getting from the p.ch.m. an estimate of the interionic QC contributions. First, the observed conformity of $\mathbf{Q}$ with the close C_{2v} symmetry of the formate ions would not be reproduced by the calculations which, second, would predict $Q_{ZZred} < Q_{ZZblue}$, contrary to what is observed. These problems disappear if we choose for the charges $q_O/e = -0.5$, $q_{Ca}/e = 1.4$, and $q_C/e = 0.3$. With this choice, the p.ch.m. leads to components $|Q_{\alpha\beta interionic}|$ ranging up to 7.7 kHz with an average of 2.4 kHz, consistent with the experimental estimate derived in the text.

The principal directions of both the blue and the red CS tensors reflect within reasonable accuracy the approximate C_{2v} symmetry of the formate ions 1 and 2. At first glance, this is a very satisfying observation. The satisfaction is, however, a complete illusion because the relations between the most, intermediate, and least shielded directions on the one hand and the C_{2v} symmetry elements of the formate ions (twofold axis, normals **n** and **n**′ of the mirror planes) on the other hand are different for ions 1 and 2. While in both ions the least shielded direction is close to **n** (deviation 6.4° (blue), 10.4° (red)), it is the most shielded direction in ion 1 but the intermediate in ion 2 which is close to the twofold axis, i.e., close to the bond (deviation 7.2° (blue), 5.3° (red)). As Post has argued and backed by magnetic point dipole calculations, the difference is caused by intermolecular shielding contributions. Our confirmation of his assignment of the CS tensors provides additional support to his calculations and conclusions. One of them is that we must accept that a proton CS tensor as it can be measured in a crystal is not always a predominantly molecular property but can reflect to a large extent the environment of the proton in the crystal.

CONCLUDING REMARKS, OUTLOOK

In this work we have explored how accurately deuteron QC and CS tensors **Q** and σ can currently be measured and where the limitations lie. The precision achieved, ±90 Hz for the components of **Q** and ±0.06 ppm for those of σ, is at least three times better than in any comparable previous experiment. Such a precision is both necessary and sufficient for demonstrating that, first, intermolecular QC contributions do play a noticeable role, their size being of the order of 4 kHz, and that, second, the unique principal QC direction at the site of a deuteron attached to a carbon need not be perfectly parallel to the bond. It is *sufficient* because at the present time the bond direction itself can be established by diffraction methods at best within, say, ±0.2°.

We point out that we used standard equipment only. Nothing was specifically designed for this experiment and this statement includes the ADC2000. It follows from the discussion of the errors that another 10-fold (!) increase of the precision of the measurement of deuteron QC tensors should be feasible. Should such a precision be aspired, it is of paramount importance to keep the tolerance level of the rotation angles of the sample crystal at around 10 arcsec. This is feasible but nonetheless a very demanding task.

We see a potential of about a factor of 2 for improving the precision of CS tensor measurements. To achieve this goal, two measures should be taken. The first is, as has become standard in line-narrowing multiple-pulse NMR (*48, 45*), to use spherical sample crystals imbedded and fixed in long cylindrical tubes. This measure eliminates the bulk susceptibility anisotropy effect upon NMR line positions. The second measure to take is to improve the phase correction of the FT spectra. Heuer's method (*34*) seeks to find a global optimum in terms of two parameters, cp and lp. Perhaps the method can be combined with a strategy

that optimizes the symmetry of each resonance locally. Unless the correct phase correction can be guaranteed within ±0.2°, an improvement of the signal/noise ratio beyond 100, as obtained in this work in single shot spectra, is meaningless.

REFERENCES

1. H. W. Spieß, *Adv. Polym. Sci.* **66,** 23 (1985).

2. M. Bloom, J. H. Davis, and M. I. Valic, *Can. J. Phys.* **58,** 1510 (1980).

3. G. L. Hoatson and R. L. Vold, *in* "NMR Basic Principles and Progress," Vol. 32, p. 1, Springer-Verlag, Berlin, 1994.

4. C. P. Slichter, "Principles of Magnetic Resonance," Chap. 6, Harper & Row, New York, 1964.

5. M. Rinné and J. Depireux, *in* "Advances in Nuclear Quadrupole Resonance," Vol. 1, p. 357, Heyden, London, 1974; see also R. G. Barnes, ibid., p. 335.

6. S. J. Kitchin and T. K. Halstead, *Appl. Magn. Reson.* **17,** 283 (1999).

7. A. Detken and H. Zimmermann, *J. Chem. Phys.* **109,** 6791 (1998).

8. D. M. Bishop and L. M. Cheung, *Phys. Rev. A* **20,** 381 (1979).

9. T. Weeding, A. L. Kwiram, D. Rawlings, and E. R. Davidson, *J. Chem. Phys.* **82,** 3516 (1985).

10. D. L. Ellis and J. L. Bjorkstam, *J. Chem. Phys.* **46,** 4460 (1967).

11. W. Derbyshire, T. C. Gorvin, and D. Warner, *Mol. Phys.* **17,** 401 (1969).

12. W. Schajor, J. Tegenfeldt, and U. Haeberlen, *J. Magn. Reson.* **44,** 285 (1981).

13. Carmen Müller, S. Idziak, N. Pislewski, and U. Haeberlen, *J. Magn. Reson.* **47,** 227 (1982).

14. Carmen Müller, W. Schajor, H. Zimmermann, and U. Haeberlen, *J. Magn. Reson.* **56,** 235 (1984).

15. S. Idziak, U. Haeberlen, and H. Zimmermann, *Mol. Phys.* **73,** 571 (1991).

16. B. Tesche, H. Zimmermann, R. Poupko, and U. Haeberlen, *J. Magn. Reson. A* **104,** 68 (1993).

17. G. Buntkowsky, W. Hoffmann, and H.-M. Vieth, *Appl. Magn. Reson.* **17,** 489 (1999).

18. H. Schlemmer and U. Haeberlen, *J. Magn. Reson.* **70,** 436 (1986).

19. F. Takusagawa, K. Hirotsu, and A. Shimada, *Bull. Chem. Soc. Jpn.* **44,** 1274 (1971).

20. D. J. Haas and S. H. Brenner, *Acta Crystallogr.* **20,** 709 (1966).

21. A. Weiss and N. Weiden, *in* "Advances in Nuclear Quadrupole Resonance," Vol. 4, table 16, p. 209, Heyden, London, 1980.

22. C. A. Michal, J. C. Wehman, and L. W. Jelinski, *J. Magn. Reson. B* **111,** 31 (1996).

23. H. Post, Ph.D. Thesis, Univ. of Heidelberg (1978).

24. H. Post and U. Haeberlen, *J. Magn. Reson.* **40,** 17 (1980).

25. I. Nitta and K. Osaki, *X-Rays* **5,** 37 (1948).

26. N. Burger, H. Fuess, and S. A. Mason, *Acta Crystallogr. B* **33,** 1968 (1977).

27. M. O. Bargouth and G. Will, *Cryst. Struct. Commu.* **9,** 605 (1980).

28. P. Speier, G. Prigl, H. Zimmermann, U. Haeberlen, E. Zaborowski, and S. Vega, *Appl. Magn. Reson.* **9,** 81 (1995).

29. The analogue part of the ADC2000 was custom-made by R. Umathum (Usoft, Heidelberg), the digital part and the software by Volker and Heike Schmitt.

30. V. Schmitt, Diplomarbeit, Univ. of Heidelberg (1989).

31. Private communication by Dr. Post from the Bruker company.

32. A. Müller, H. Zimmermann, and U. Haeberlen, *J. Magn. Reson.* **126,** 66 (1997).

33. B. G. Segal, M. Kaplan, and G. K. Fraenkel, *J. Chem. Phys.* **43,** 4191 (1965).

34. A. Heuer, *J. Magn. Reson.* **91,** 241 (1991).

35. D. Gross, N. Pislewski, U. Haeberlen, and K. H. Hausser, *J. Magn. Reson.* **54,** 236 (1983).

36. A. Heuer and U. Haeberlen, *J. Magn. Reson.* **85,** 79 (1989).

37. G. M. Volkoff, *Can. J. Phys.* **31,** 820 (1953).

38. S. Dusold and Angelika Sebald, *Mol. Phys.* **95,** 1237 (1998).

39. A. Abragam, "The Principles of Nuclear Magnetism," Chap. VII, Oxford Univ. Press, London, 1961.

40. LANDOLT-BÖRNSTEIN, Part 10, Vol. II, p. 12, Springer-Verlag, Berlin, 1967.

41. G. Soda and T. Chiba, *J. Phys. Soc. Japan* **26,** 249 (1969).

42. M. Da Graca, C. Dillon, and J. A. S. Smith, *J. Chem. Soc. Faraday Trans. II* **68,** 2183 (1972).

43. G. J. Adriaenssens and J. L. Bjorkstam, *J. Chem. Phys.* **56,** 1223 (1972).

44. T. Weeding, A. L. Kwiram, D. C. Rawlings, and E. R. Davidson, *J. Chem. Phys.* **82,** 3516 (1985).

45. B. Tesche, Ph.D. Thesis, University Heidelberg (1995).

46. T. Bräuninger, R. Poupko, Z. Luz, P. Gutsche, C. Meinel, H. Zimmermann, and U. Haeberlen, *J. Chem. Phys.* **112,** 10858 (2000).

47. A. M. Achlama and Y. Zur, *J. Magn. Reson.* **36,** 249 (1979).

48. R. Prigl and U. Haeberlen, *Adv. Magn. Opt. Reson.* **19,** 1 (1996).